Journal of Microbiology, Immunology and Infection 56 (2023) 1026–1035

Available online at www.sciencedirect.com

ScienceDirect

journal homepage: www.e-jmii.com

Original Article

Isolation and characterization of bacteriophages with activities against multi-drug-resistant *Acinetobacter nosocomialis* causing bloodstream infection *in vivo*

Ho Yin Pekkle Lam [a], Meng-Jiun Lai [b], Wen-Jui Wu [b], Ying-Hao Chin [c], Huei-Jen Chao [c], Li-Kuang Chen [c], Shih-Yi Peng [a,], Kai-Chih Chang [b,c,*]**

[a] *Department of Biochemistry, School of Medicine, Tzu Chi University, Hualien, Taiwan*
[b] *Department of Laboratory Medicine and Biotechnology, Tzu Chi University, Hualien, Taiwan*
[c] *Department of Laboratory Medicine, Hualien Tzu Chi Hospital, Buddhist Tzu Chi Medical Foundation, Hualien, Taiwan*

Received 23 February 2023; received in revised form 4 July 2023; accepted 31 July 2023
Available online 5 August 2023

KEYWORDS
Acinetobacter nosocomialis;
Bacteriophages;
Myoviridae;
Podoviridae

Abstract *Background: Acinetobacter nosocomialis* (*A. nosocomialis*) is a glucose non-fermentative, gram-negative bacillus that belongs to the *Acinetobacter calcoaceticus-baumannii* complex. In recent years, studies have found an increased clinical prevalence of *A. nosocomialis*. However, given the increasing trend of antibiotic resistance, developing new antibacterial agents is vital. Currently, research regarding bacteriophage therapy against *A. nosocomialis* is only limited.
Methods: Two *A. nosocomialis* bacteriophages, TCUAN1 and TCUAN2, were isolated from sewage. Experiments such as transmission electron microscopy (TEM), host-range analysis, and sequencing were performed to determine their biological and genomic characteristics. TCUAN2 were further subjected to *in vivo* experiments and their derived-endolysin were cloned and tested against their bacteria host.
Results: Transmission electron microscopy revealed that TCUAN1 and TCUAN2 belong to *Myoviridae* and *Podoviridae*, respectively. Both phages show a broad host spectrum and rapid adsorption efficiency. Further biological analysis showed that TCUAN2 possesses a shorter latent period and larger burst size compared to TCUAN1. Because TCUAN2 showed a better antibacterial activity, it was injected into *A. nosocomialis*-infected mice which resulted in a

** Corresponding author. Department of Biochemistry, School of Medicine, Tzu Chi University, No. 701, Zhongyang Rd., Sec 3, Hualien 970, Taiwan.
* Corresponding author. Department of Laboratory Medicine and Biotechnology, Tzu Chi University, No. 701, Zhongyang Rd., Sec 3, Hualien 970, Taiwan. Fax: +886 3 857-1917.
E-mail addresses: pengsy@mail.tcu.edu.tw (S.-Y. Peng), kaichih@mail.tcu.edu.tw (K.-C. Chang).

https://doi.org/10.1016/j.jmii.2023.07.012

significant decrease in bacterial load levels in the blood and increased the mice's survival. Finally, genomic analysis revealed that the complete nucleotide sequence of TCUAN1 is 49, 691 bps (containing 75 open reading frames) with a G + C content of 39.3%; whereas the complete nucleotide sequence of TCUAN2 is 41, 815 bps (containing 68 open reading frames) with a G + C content of 39.1%. The endolysin gene cloned and purified from TCUAN2 also showed antibacterial activity when used with a chelator EDTA.

Introduction

Acinetobacter nosocomialis (*A. nosocomialis*) is a glucose non-fermenting and non-motile gram-negative coccobacillus.[1] Although ubiquitous in the natural environment, it can also be an opportunistic pathogen to immunocompromised patients, causing pneumonia, wound infections, and septicemia.[2,3] Therefore, *A. nosocomialis* is known as a pathogenic member of the *Acinetobacter calcoaceticus-baumannii* complex.[4–6] Before the development of advanced diagnostic techniques, *Acinetobacter baumannii* was identified as the bacteria responsible for most nosocomial infections.[7,8] Yet, more recent evidence suggest that *A. nosocomialis* is also frequently isolated in the clinical setting.[9–11] Together, *A. baumannii* and *A. nosocomialis* account for more than 80% of all *Acinetobacter* infections in Taiwan.[11,12]

Currently, the most commonly used agents for *Acinetobacter* infections include carbapenems, polymyxins, sulbactam, tigecycline, and aminoglycosides.[13,14] However, *Acinetobacter* usually presents resistance to multiple antibacterial agents (multidrug-resistant or pandrug-resistant). Several studies have reported clinical isolation of multi-drug-resistant *Acinetobacter*, with carbapenem resistance in a growing trend.[15–18] Given the increasing crisis of multidrug resistance, developing new alternative agents against *Acinetobacter* is imperative.

Bacteriophage therapy is one of the most promising antibacterial agents in recent years.[19–22] Bacteriophages specifically target the bacterial host with only minimal impact on the normal microbial flora.[23,24] Furthermore, unlike chemical antibiotics, bacteriophages were derived from the natural environment, therefore, they have a relatively low environmental impact.[25,26] More importantly, bacteriophages were effective against multidrug-resistant bacteria both *in vivo* and *in vitro*.[27,28] Bacteriophage therapy has also been clinically applied to humans in treating gas gangrene,[29] bacterial dysentery,[30–32] and multi-drug-resistant *A. baumannii* infection.[19]

Many attempts have been made to find *A. baumannii* bacteriophages, but only limited evidence was addressed in finding bacteriophages against *A. nosocomialis*. Therefore, this study will aim to isolate and characterize bacteriophages against *A. nosocomialis*.

Materials and methods

Bacterial strains and culture conditions

Thirty-three *A. nosocomialis* clinical isolates and ten *A. baumannii* clinical isolates were collected from Hualien Tzu Chi Hospital, Hualien, Taiwan. The *A. baumannii* reference strain ATCC 17978 was obtained from Bioresource Collection and Research Center (BCRC), Hsinchu, Taiwan. All clinical isolates were confirmed as *A. nosocomialis* or *A. baumannii* by matrix-assisted laser desorption ionization-time of flight (MALDI-TOF) and are multidrug resistant. The sources of the bacteria strain used in this study are listed in Supplementary Table 1. All bacterial cultures were grown on Luria Bertani (LB) broth or LB agar at 37 °C.

Bacteriophage isolation and propagation

Sewage samples were collected from Hualien Sewage Treatment Plant, Hualien, Taiwan, and Hualien Tzu Chi Hospital, Hualien, Taiwan. The sewage samples were centrifuged at 10,000×*g* for 10 min, and the supernatants were passed through a filter with a 0.45 μm pore size. To enrich the phage, a 1-mL culture of *A. nosocomialis* strains (mixture of different strains; OD_{600} = 1.0) was inoculated with 40 mL of sewage filtrate and incubated at 37 °C for 18 h. The mixtures were centrifuged at 10,000×*g* for 10 min and filtered through 0.45 μm filters to remove residual bacterial cells. Subsequently, phages were identified by the double-layer agar method which was incubated at 25 °C. After confirming the presence of plaque on the agar, a single plaque was picked using a sterile pipette tip and inoculated in a new culture. The procedure was repeated several times for bacteriophage purification. Purified phages were then stored at 4 °C or −80 °C in 30% (v/v) glycerol until further experiments.

Based on the double-layer agar analysis, YPL18 and TCH_Bab001_050 were chosen as the most suitable host bacteria for TCUAN1 and TCUAN2, showing the best infection efficiency for the phages.

Host range determination

The host range was determined by the spot method and confirmed with the double-layer agar method on the *A.*

nosocomialis and *A. baumannii* strains listed in Supplementary Table 1. The spot method was done by spreading the bacteria on the LB agar with a sterile cotton swab, followed by spotting 10 μL phage lysate (10^9 PFU/mL) onto the bacterial lawns. The presence of lytic zone (plaque) was observed after incubating the agar at 25 °C overnight. A double-layer agar method was performed by mixing 100 μL of *A. nosocomialis* (in the log phase), 1 mL serially diluted phage lysates, and 5 mL 0.6% LB soft agar medium together. The mixture was then overlaid onto the 1.2% LB agar. The plates were incubated at 25 °C overnight and observed for the presence of plaque.

Transmission electron microscopy (TEM) analysis

Phage lysate (10^9 PFU/mL) was placed on a freshly prepared formvar-coated grid (200 mesh copper grids), followed by negative staining with 2% uranyl acetate. The morphology of bacteriophages was observed with a Hitachi H-7500 transmission electron microscope (Hitachi Company, Japan) at an acceleration voltage of 80 kV.

Determination of phage multiplicity of infection (MOI)

To determine the multiplicity of infection (MOI), the host strain was grown in LB broth until it reached the early log phase (OD_{600} = 0.5). The phages were added at different MOI from 0.0001 to 100, and the mixtures were incubated at 37 °C for 3 h. After centrifugation at 10,000×*g* for 10 min, the supernatants were serially diluted, and the phage titer was determined by the double-layer agar method.

Adsorption assay

After the bacteria reached OD_{600} = 1, it was mixed with the phage suspension to achieve MOI = 0.01 in the total volume of 20 mL. The mixtures were then incubated at 37 °C, and 1 mL samples were taken every 2 min for a total of 10 min. The samples were centrifuged at 10,000×*g* for 5 min, followed by a serial dilution of the supernatant. After that, the un-adsorbed phages were determined by the double-layer agar method.

One-step growth curve assay

To determine the latent period and the burst period of the isolated phages, 3 mL of bacterial culture (OD_{600} = 1) was mixed with phage (MOI = 0.01). The samples were incubated at 4 °C for 10 min to facilitate adsorption. The mixture was then centrifuged, resuspended in 30 mL phage buffer (10 mM Tris—HCl, 10 mM $MgSO_4$, 68.5 mM NaCl, 1 mM $CaCl_2$, pH 7.5), and incubated at 25 °C. A 1 mL sample was taken every 10 min, serially diluted, and plated by the double-layer agar method.

Infection assay

Once the bacteria reached OD_{600} = 0.5, phages at different MOI (from 0.0001 to 10) were added and incubated at 37 °C. Bacteria growth was monitored over time by measuring OD_{600} at a 30 min interval for the first 4 h, followed by 1 h interval for 4 h.

Genome sequencing and bioinformatic analysis

Total genomic DNA of bacteriophages was extracted as described previously.[33] Whole-genome sequencing of the phage DNA was performed using the Oxford Nanopore MinION Mk1C (Oxford, United Kingdom). Prediction of all open reading frames (ORFs) was done by Prodigal, and annotation of predicted ORFs was carried out by the Basic Local Alignment Search Tool (BLAST). The sequence data and annotation information of phage TCUAN1 and TCUAN2 were deposited at GenBank under accession numbers ON531988 and ON531987, respectively.

Phage therapy against *A. nosocomialis* infection in mice

Twelve five-week-old male BALB/c mice (National Laboratory Animal Center, Taipei, Taiwan) were randomly divided into two groups, each containing six mice. All mice were first intraperitoneally infected with 10^9 CFU/mL *A. nosocomialis* suspended in sterile saline. Ten minutes later the mice were intraperitoneally injected with 150 μL sterile saline or 150 μL TCUAN2 suspension (containing 10^{10} PFU/mL). Blood was drawn from the tail vein of mice 3 h after phage injection. The collected blood was evenly smeared on LB agar and incubated at 37 °C for 18 h. The number of bacterial colonies was counted. All protocols involving animals were approved by the Institutional Animal Care and Use Committees (IACUC) of Tzu Chi University (No. 107083).

Cloning, expression, and purification of LysAN2

The ORF_61 (LysAN2) was predicted to encode an endolysin protein in TCUAN2. This region was amplified by PCR with primer specific for ORF_61: LysAN2-Fp (5′-GGATCC GTG GAG AAA TCT ACT GAG T-3′) and LysAN2-Rp (5′-GTCGACC-TAGTGCCT TTCGG-3′). The amplified products were ligated into a pGEM-T easy vector (Promega, WI, USA). The recombinant DNA was then digested with *Eco*RI (New England Biolabs, MA, USA) and cloned into the pET-30a expression vector (Novagen, WI, USA). The resulting construct pET30a-*lysAN2*, after being confirmed by DNA sequencing, was transformed into competent *Escherichia coli* BL21 (DE3) for protein expression. *E. coli* BL21 (DE3) harboring the pET30b-*lysAN2* were inoculated into LB broth containing 50 μg/mL kanamycin and incubated at 37 °C until an OD_{600} = 0.6 was reached. The protein expression was induced by adding 0.1 mM isopropyl-β-D-1-thiogalactopyranoside (IPTG) followed by incubation at 37 °C for 3 h. Cultures were centrifuged at 10,000×*g* for 10 min. The remaining pellets were resuspended in 3 mL of

lysis-equilibration-wash (LEW) buffer (50 mM NaH_2PO_4, 300 mM NaCl, pH 8.0), lysed by sonication, and centrifuged at 10,000×*g* for 10 min to remove cellular debris. The supernatant lysate was purified by a Protino Ni-TED column (MACHEREY-NAGEL, Düren, Germany). The eluted protein was confirmed on a 12% SDS-PAGE and the concentration was determined by Bradford assay.

Antibacterial activity of LysAN2

The antibacterial activity of LysAN2 was examined by calculating bacterial survival as described previously.[34] Briefly, *A. baumannii* or *A. nosocomialis* were grown overnight in a 10 mL LB medium to reach their stationary phase. Two-hundred microliter of the overnight culture was inoculated into a 10 mL LB medium, allowing the bacteria to grow for 4 h to exponential phase. Bacteria from the exponential phase cultures were washed and resuspended in sterile water to create bacterial cultures at a density of $OD_{600} = 1$. One-hundred microliter (containing 2×10^6 CFU/mL) culture was added into an Eppendorf. Subsequently, 100 μL of sterile water, each singly and in combination, containing 0.5 mM EDTA, 200 μg/mL LysAN2, or 200 μg/mL lysozyme were added into the same Eppendorf tube. One hour later the bacteria were plated on LB agar and their CFUs were determined. The CFUs in the treated groups were normalized to the CFUs in the control group.

Results

Isolation of bacteriophages and their morphologic characteristics

Using 33 clinical isolates of *A. nosocomialis*, two bacteriophages were isolated from the sewage. These two phages were named TCUAN1 and TCUAN2, respectively. Both phages produce similar plaques with a turbid halo (Fig. 1A). Transmission electron microscopy (TEM) analysis revealed that both TCUAN1 and TCUAN2 possess an icosahedron head with a diameter of 91.0 ± 15.6 nm and 79.0 ± 8.2 nm, respectively. TCUAN1 also possesses a long tail of about 120.0 ± 7.9 nm, whereas TCUAN2 includes only a short tail of about 8.0 ± 4.5 nm. Therefore, according to the appearance of the phages, TCUAN1 may belong to *Myoviridae* while TCUAN2 to *Podoviridae* (Fig. 1B).

Host range analysis showed that TCUAN1 could infect nine out of 33 clinical isolates of multidrug resistant *A. nosocomialis*. In contrast, TCUAN2 could infect eight out of 33 multi-drug-resistant *A. nosocomialis* and three clinical isolates of multi-drug-resistant *A. baumannii* (Fig. 1C).

Biological characterization of TCUAN1 and TCUAN2

To study the optimal multiplicity of infection (MOI), TCUAN1 was tested against their host from MOI = 0.01 to MOI = 100, and TCUAN2 was tested from MOI = 0.0001 to MOI = 1. The results showed that the optimal MOI for TCUAN1 was MOI = 10 (Fig. 2A) and TCUAN2 was MOI = 0.01 (Fig. 2B); both could yield a phage titer of about 10^{10} PFU/mL. To investigate the adsorption rate of TCUAN1 and TCUAN2, the phages were infected with their host strains at an MOI of 0.01. The results showed that both TCUAN1 and TCUAN2 possess rapid adsorption efficiency, with more than 90% of phages being absorbed into their host strains within 4 min. The adsorption rate for both phages was more than 98% (Fig. 2C and D). By infecting the phages with their host strains, the growth curve showed that the latent period of TCUAN1 and TCUAN2 was about 30 min and 5 min, respectively. TCUAN1 could release about 47 phage particles per infected bacterial cell, while TCUAN2 could release about 64 phage particles per infected cell (Fig. 2E and F). In TCUAN1 and TCUAN2, the burst size went down steeply after 50 min and 10 min, which may be because the phage is again reabsorbed into the bacterial cells and ready for another round of bursts (Fig. 2E and F).

Infection ability of TCUAN1 and TCUAN2

To investigate the ability of TCUAN1 and TCUAN2 to inhibit bacterial growth, the two phages were infected with their host at different MOIs. The results suggested that TCUAN1 showed a relatively weak inhibitory effect and could only temporarily inhibit bacterial growth (Fig. 3A). On the other hand, TCUAN2 has a significantly better infection ability compared to TCUAN1. An MOI as low as 0.0001 can still effectively inhibit bacteria growth, which persists for 480 min (Fig. 3B).

Genome analysis of TCUAN1 and TCUAN2

Whole-genome sequence analysis of TCUAN1 and TCUAN2 was performed using the Oxford Nanopore MinION Mk1C (Oxford, United Kingdom). The genome of TCUAN1 contains 49,691 bp with a G + C content of 39.3%; whereas the TCUAN2 genome contains 41,815 bp with a G + C content of 39.1%. Annotation of the ORF showed that TCUAN1 and TCUAN2 contain 75 and 68 predicted ORFs, respectively (Fig. 4A and B; Supplementary Tables 2 and 3). Of the 75 predicted ORFs in TCUAN1, 22 ORFs were predicted as functional proteins while 53 ORFs were hypothetical proteins (Fig. 4A; Supplementary Table 2). For TCUAN2, 41 ORFs were predicted as functional proteins and 27 ORFs as hypothetical proteins (Fig. 4B; Supplementary Table 3). Based on BLASTn alignments, TCUAN1 was found to share 93% sequence similarity with an *A. baumannii* phage AB11510-phi (GenBank: MT361972.1) but with only 12% query coverage. On the other hand, TCUAN2 revealed a high degree of sequence identity between the two reported *A. baumannii* phages, phiAB1 (GenBank: HQ186308.1) and phiAB6 (GenBank: KT339321.1), with a 95.8% and 95.7% sequence similarity and a query coverage of more than 88%.

In vivo phage therapy in antibiotic-resistant *A. nosocomialis* infected-mice

TCUAN2 showed better infection ability to the host than TCUAN1. TCUAN2 also presented a broader host range, infecting both *A. nosocomialis* and *A. baumannii*. Therefore, TCUAN2 was chosen to analyze its effectiveness in the treatment of *A. nosocomialis*-infected mice. The results

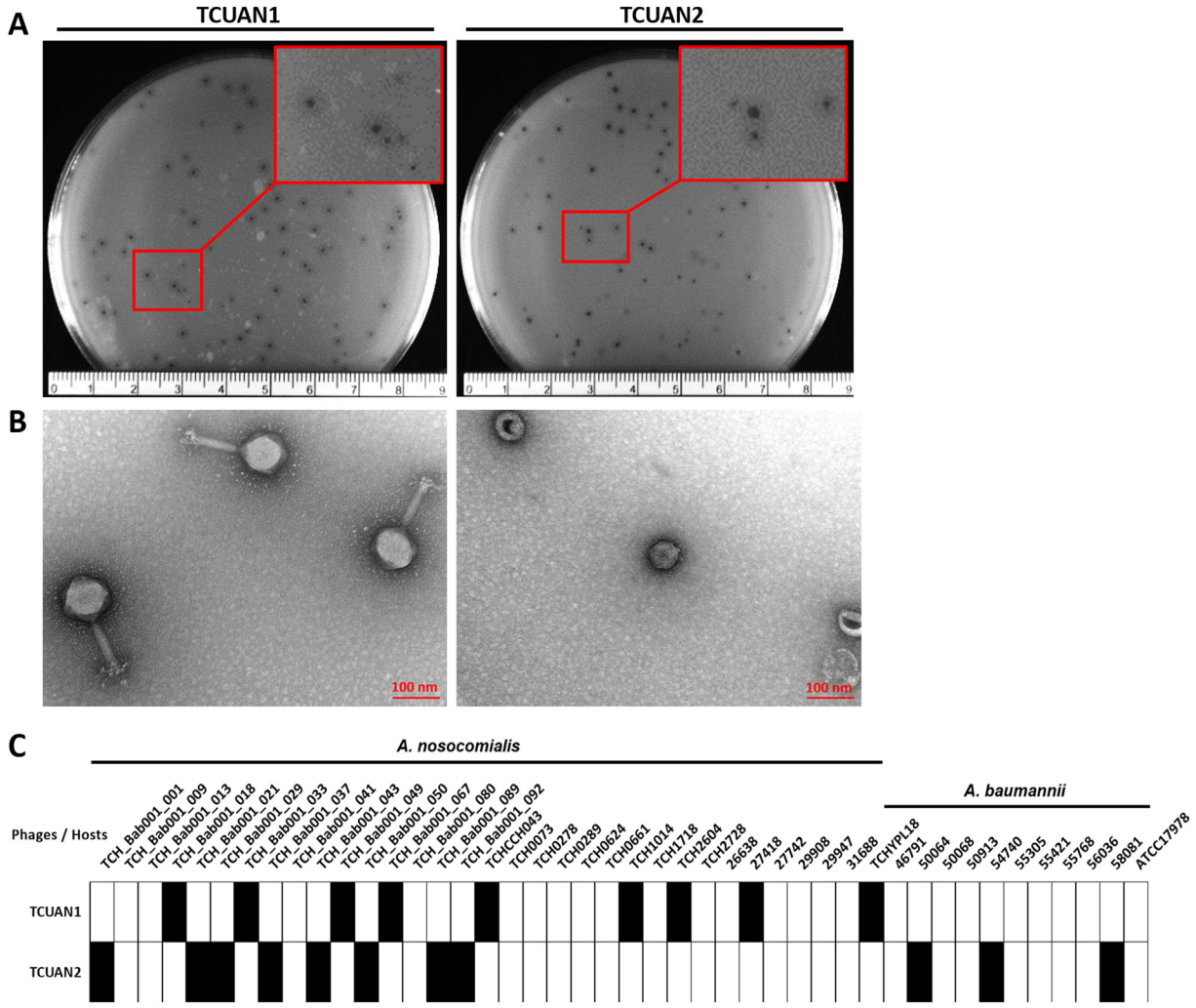

Figure 1. Virion morphology and host range of TCUAN1 and TCUAN2. (A) Representative images of phage morphology identified by the double-layer agar. Both phages produce similar plaques with a turbid halo. (B) Representative transmission electron microscopic (TEM) image of the phages. TCUAN1 possesses an icosahedron head and a thick and long tail, whereas TCUAN2 possesses an icosahedron head and a short tail. The scale bar indicates 100 μm. (C) The host range of TCUAN1 and TCUAN2. White cells represent no lysis to the bacterial host and black cells represent lysis to the bacterial host.

showed that the bacterial count in the blood of the non-treated group was 30 × 10^4 CFU/mL; while the bacterial count in the treatment group was 1000 times less than the non-treated group, giving an average bacterial count of 300 CFU/mL (Fig. 5A). In addition, TCUAN2 significantly increase the mice's survival (Fig. 5B). These results therefore suggested that TCUAN2 may be beneficial to use as a therapeutic against infection of antibiotic-resistant *A. nosocomialis*.

Antibacterial activity of the putative endolysin LysAN2

As the antibacterial activity may be related to the bacteriophage's endolysin,[35] we next investigate whether the endolysin cloned from TCUAN2 may possess the expected antibacterial activity. ORF_61 in TCUAN2 was predicted to encode an endolysin protein (Supplementary Table 3). The endolysin cloned and purified from TCUAN2 was named LysAN2. Antibacterial activity of LysAN2 (at a concentration of 200 ug/mL was tested against the host of TCUAN2, TCH_B001_050, and an *A. baumannii* strain, ATCC17978. While lysozyme was used as a positive control, EDTA was used as a chelator, which can disrupt the bacterial membrane and facilitate the effect of endolysin.[35,36] Interestingly, the sole use of LysAN2 induced a higher survival of *A. nosocomialis* (Fig. 6A); whereas it inhibited the survival of *A. baumannii* (Fig. 6B). Yet, combination of LysAN2 and EDTA inhibited the survival of both *A. nosocomialis* and *A. baumannii*. The increased bacterial survival by LysAN2 was further confirmed by measuring the OD_{600} value of a growing TCH_B001_050 broth (Supplementary Fig. 1A). Furthermore, the induction of bacteria growth was also

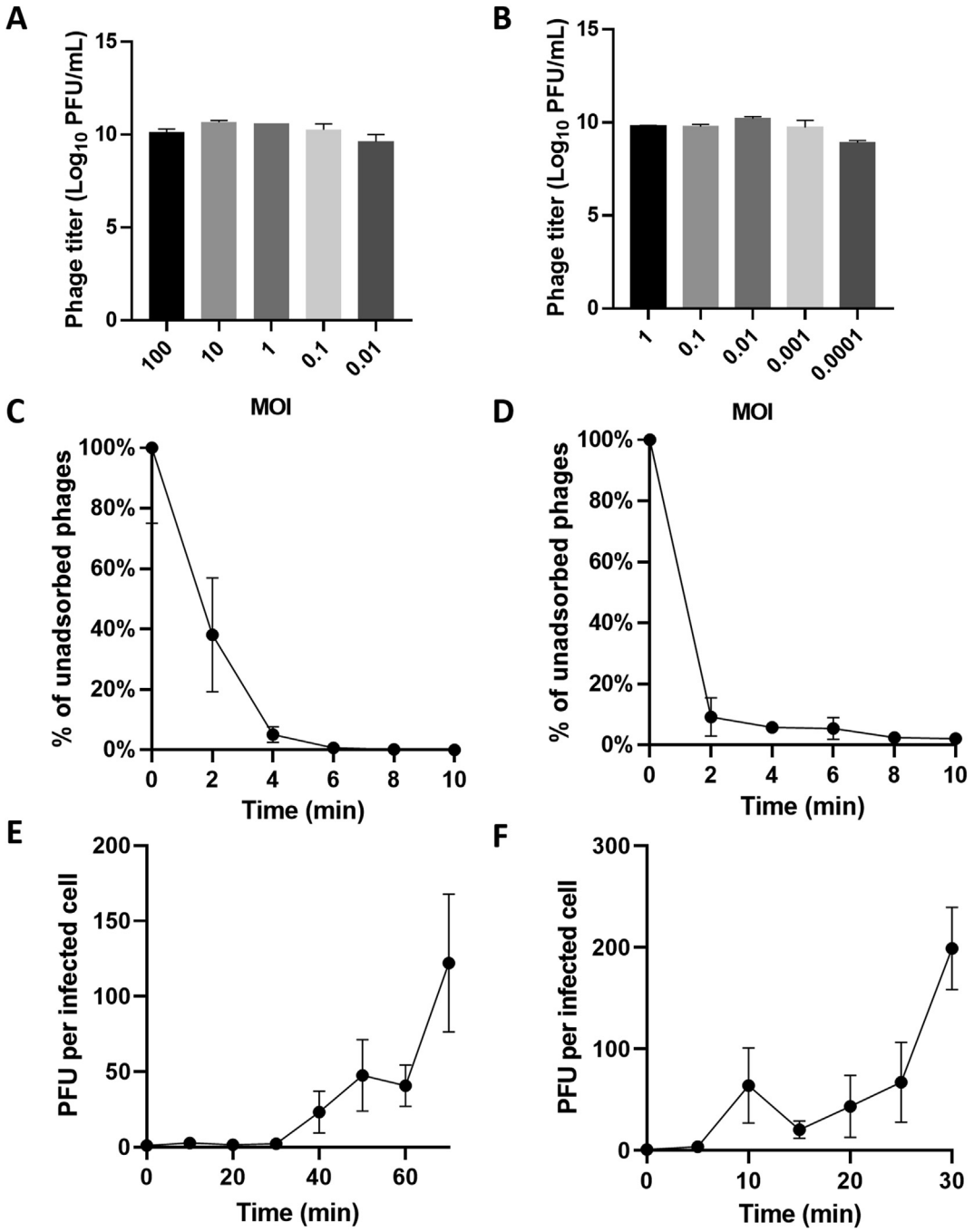

Figure 2. Biological characteristics of TCUAN1 and TCUAN2. The optimal multiplicity of infection (MOI) of (A) TCUAN1 and (B) TCUAN2 was determined by infecting the phage with its host. Adsorption curve of (C) TCUAN1 and (D) TCUAN2 to their bacterial host at MOI = 0.01. The percentage of unabsorbed phages was calculated by dividing the phage titer in the supernatant by that in the initial phage stock. One-step growth curve of (E) TCUAN1 and (F) TCUAN2.

observed in other *A. nosocomialis* strains (Supplementary Fig. 1B), suggesting that our observation was not a coincidence.

Discussion

Prior to the development of advanced molecular techniques, many *Acinetobacter* species with phenotypic characteristics similar to *A. baumannii* had been misidentified.[9] Recent evidence found that *A. nosocomialis*, in addition to *A. baumannii*, was also the pathogen that led to human infections.[8] Given the upward trend of drug-resistant *Acinetobacter*, phage therapy may be considered one of the promising antibacterial agents.[11,15,17]

In the present study, we successfully isolated two *A. nosocomialis* phages from sewage, which were designated as TCUAN1 and TCUAN2. TEM analysis indicated that

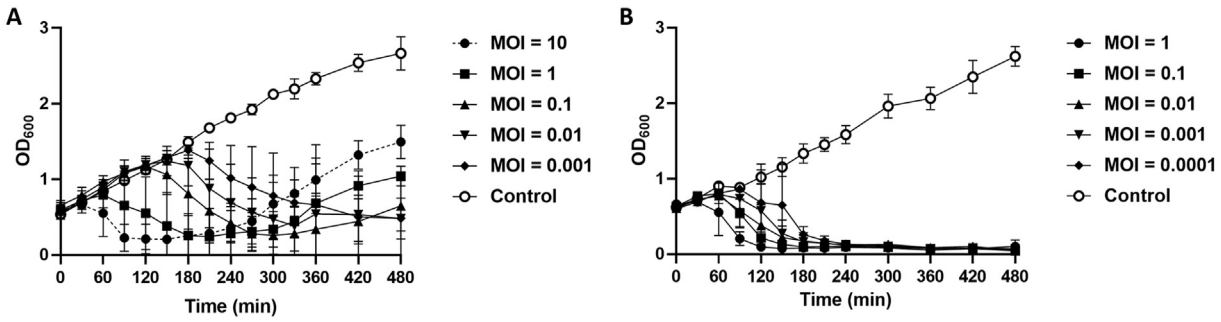

Figure 3. Infection assay of TCUAN1 and TCUAN2. Infection assay of (A) TCUAN1 and (B) TCUAN2. TCUAN2 showed a better host growth inhibitory ability compared to TCUAN1.

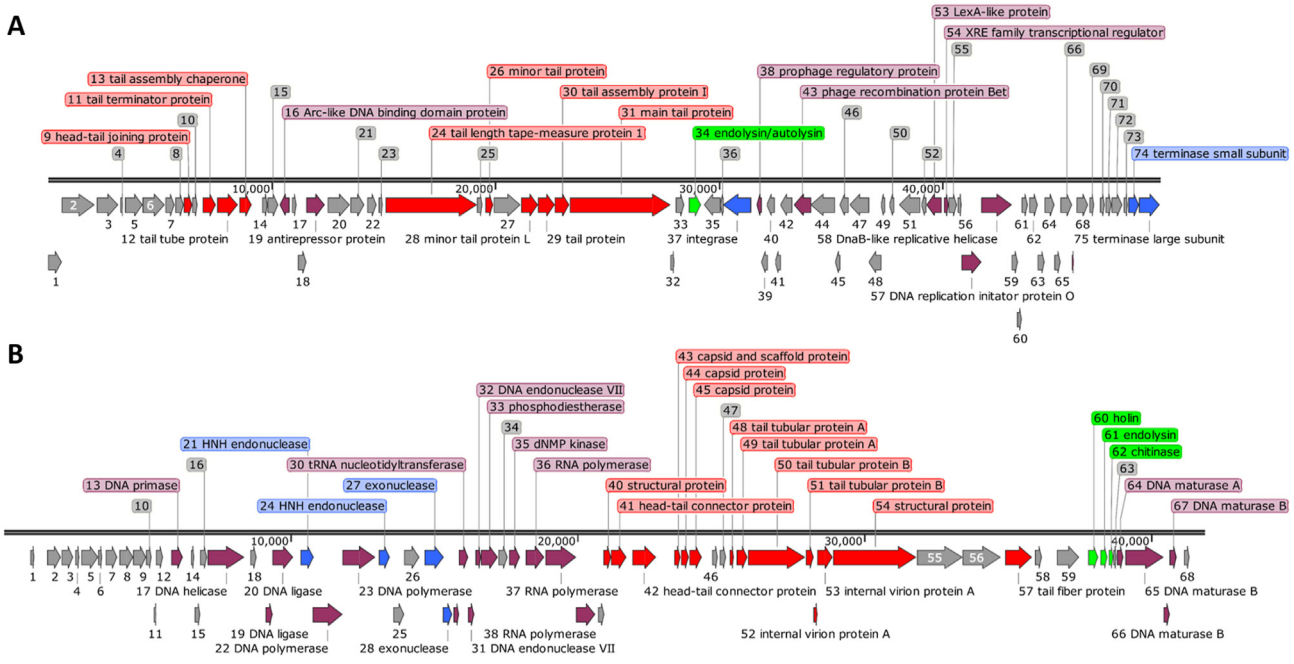

Figure 4. Genomic organization of TCUAN1 and TCUAN2. (A) TCUAN1 contains 49,691 bps and 75 predicted open reading frames (ORFs). (B) TCUAN2 contains 41,815 bps and 68 predicted ORFs. ORFs coding for structural proteins are marked in red; DNA packaging proteins are marked in blue; lytic proteins are marked in green; proteins involved in DNA replication are marked in magenta; hypothetical proteins are marked in grey. The figure was generated using the SnapGene program, http://www.snapgene.com (accessed on 26 June 2022).

TCUAN1 belongs to *Myoviridae* and TCUAN2 belongs to *Podoviridae*. Further phylogenetic analysis from the genome sequence of DNA polymerase confirmed that TCUAN2 belongs to *Podoviridae* (Supplementary Fig. 2). However, because of the lack of information on the DNA polymerase genome in TCUAN1 (Supplementary Table 2), phylogenetic analysis was done using other predicted ORF such as endolysin or tail protein; the results showed similarity to *Actinobacter* genome but, when restricted to only *Myoviridae*, only one possible *Actinobacter* phage genome (GenBank accession number: YP_009289791.1; data not shown). Because TCUAN1 was the first bacteriophage discovered that is highly selective to *A. nosocomialis* (Fig. 1C), knowledge regarding this phage is far from complete, as many discovered *Actinobacter* phages were identified as *A. baumannii* phages. On the other hand, TCUAN2 had a border host range than TCUAN1 and can infect some strains of *A. baumannii* (Fig. 1C). Although both TCUAN1 and TCUAN2 showed rapid adsorption efficiency, TCUAN2 had a better infection ability than TCUAN1.

Further research revealed that TCUAN2 is morphologically similar to Petty (GenBank accession number KF669656.1), another bacteriophage that can infect *A. nosocomialis*, which both of them belong to *Podoviridae* and form plaques with a translucent halo.[37] However, Petty had a longer latent period and larger burst size (240 PFU/infected cell)[37] while TCUAN2 had a shorter latent period but smaller burst size (64 PFU/infected cells). Studies have reported that the growth and replication of phages with a long latent period can be time-consuming and inefficient, whereas phages with a short latency may replicate more quickly and can effectively release progeny phages.[38] Since TCUAN1 has a long

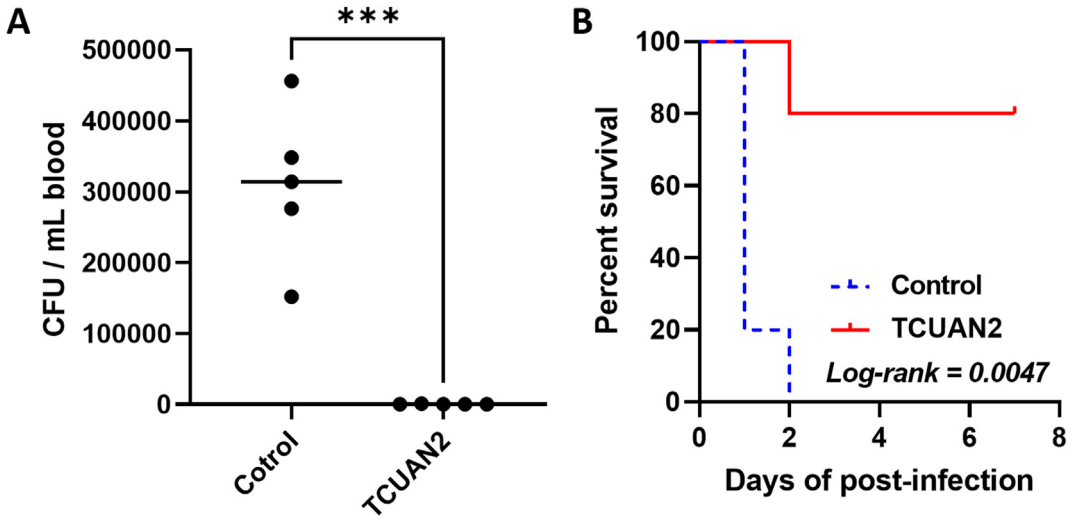

Figure 5. TCUAN2 decrease bacterial load in *A. nosocomialis*-infected mice. Bacterial load of *A. nosocomialis* in the blood of *A. nosocomialis*-infected mice. The mice were intraperitoneally injected with 10^9 CFU/mL *A. nosocomialis*. Ten minutes later, the mice were intraperitoneally injected with 150 μL sterile saline (control group) or 10^{10} PFU/mL TCUAN2. Blood was drawn from the tail vein of mice 3 h post-phage injection. The collected blood was evenly smeared on LB agar and incubated at 37 °C for 18 h. Significance determined by t-test. (A) The CFU of bacteria in the blood. (B) Survival difference was observed between the two groups. Significance was determined by log-rank test.

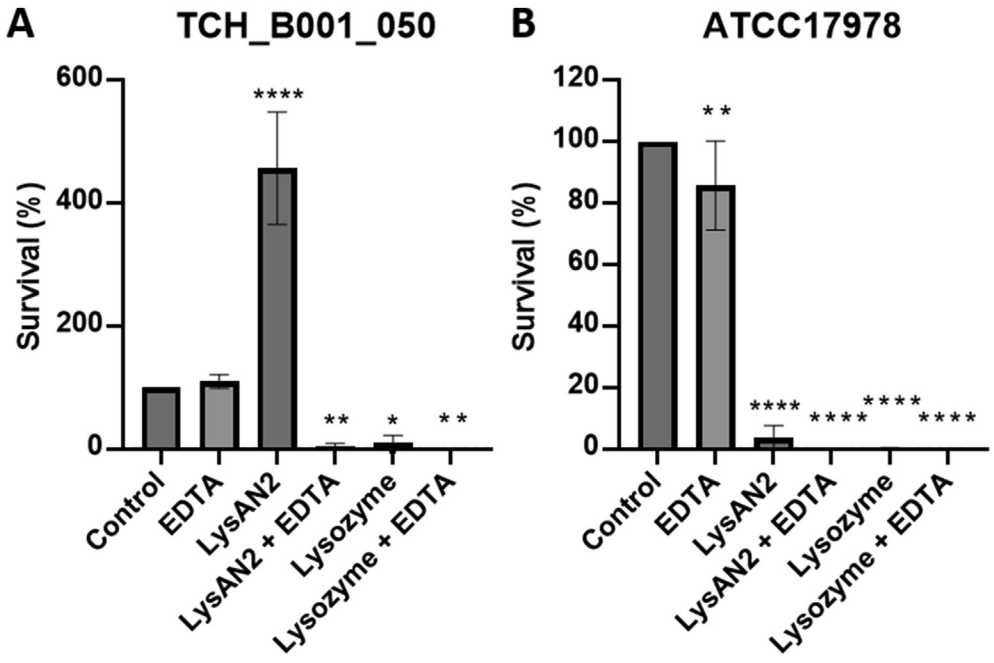

Figure 6. Putative endolysin LysAN2 processes an antibacterial activity against *A. nosocomialis* and *A. baumannii*. Bacterial survival after LysAN2 treatment on (A) *A. nosocomialis* and (B) *A. baumannii*. *$p < 0.05$; **$p < 0.01$; and ****$p < 0.0001$. Significance determined by one-way ANOVA.

latent period and smaller burst size than TCUAN2, it may be the reason for its slower infection ability.

The therapeutic effect of TCUAN2 was next investigated on multidrug-resistant *A. nosocomialis*-infected mice. TCUAN2 effectively reduces the number of bacteria in the blood and increases the mice's survival (Fig. 5). Herein, our findings demonstrated the potential of phage therapy as an additional tool to antibiotic treatments, given the growing antibiotic resistance. Furthermore, the combined use of TCUAN2 with current antibiotics on antibiotic-sensitive strains may reduce the emergence of phage-resistant and antibiotic-resistant strains, which could serve as a continuous incentive for future studies.

Bacteriophage-derived endolysin is considered to be another alternative for the treatment of bacterial infections.[39—42] Our results suggested that LysAN2

combined with EDTA showed suitable bactericidal activities against *A. nosocomialis* and *A. baumannii*. However, the sole use of LysAN2 can only inhibit the growth of *A. baumannii* but not *A. nosocomialis*. This can be explained by the partial hydrolytic activity of LysAN2 against the peptidoglycan of the bacterial cell wall, thereby enhancing bacterial fission, as normal bacterial replication requires autolysis of the bacterial cell wall.[43] The use of EDTA can disrupt the bacterial membrane,[35] which synergizes the activity of LysAN2, leading to bacterial death. This result, however, suggests that the safety of the use of bacteriophages-derived endolysin may need to be considered in the future. Yet, combining endolysin with other antibiotics or drugs may be useful to overcome this safety issue.

Nevertheless, TCUAN2 and their endolysin products, in addition to *A. nosocomialis*, are also effective in killing some strains of the *A. baumannii* (Figs. 1C and 6B), this may therefore as well show promise in treating *A. baumannii* infections.

In conclusion, our study represents two new bacteriophages against *A. nosocomialis*, TCUAN1 and TCUAN2. Our *in vitro* and *in vivo* results are encouraging that TCUAN2 or their derived products may be a promising therapeutic option against multidrug-resistant *A. nosocomialis*.

Declaration of competing interest

All authors declare that they have no conflict of interest.

Acknowledgments

This work was supported partly by grants TCU-B01 from Tzu Chi Foundation, Taiwan and partly by the grants 110-2320-B-320-005-MY3 from the Ministry of Science and Technology of Taiwan. We thank the Electron Microscopy Laboratory of the Department of Anatomy of Tzu Chi University for technical assistance.

References

1. Bergogne-Berezin E, Towner KJ. Acinetobacter spp. as nosocomial pathogens: microbiological, clinical, and epidemiological features. *Clin Microbiol Rev* 1996;**9**:148—65.
2. Towner KJ. Acinetobacter: an old friend, but a new enemy. *J Hosp Infect* 2009;**73**:355—63.
3. Wang X, Chen T, Yu R, Lu X, Zong Z. Acinetobacter pittii and Acinetobacter nosocomialis among clinical isolates of the Acinetobacter calcoaceticus-baumannii complex in Sichuan, China. *Diagn Microbiol Infect Dis* 2013;**76**:392—5.
4. Gerner-Smidt P, Tjernberg I, Ursing J. Reliability of phenotypic tests for identification of Acinetobacter species. *J Clin Microbiol* 1991;**29**:277—82.
5. Nemec A, Krizova L, Maixnerova M, van der Reijden TJ, Deschaght P, Passet V, et al. Genotypic and phenotypic characterization of the Acinetobacter calcoaceticus-Acinetobacter baumannii complex with the proposal of Acinetobacter pittii sp. nov. (formerly Acinetobacter genomic species 3) and Acinetobacter nosocomialis sp. nov. (formerly Acinetobacter genomic species 13TU). *Res Microbiol* 2011;**162**:393—404.
6. Tjernberg I, Ursing J. Clinical strains of Acinetobacter classified by DNA-DNA hybridization. *APMIS* 1989;**97**:595—605.
7. Turton JF, Shah J, Ozongwu C, Pike R. Incidence of Acinetobacter species other than A. baumannii among clinical isolates of Acinetobacter: evidence for emerging species. *J Clin Microbiol* 2010;**48**:1445—9.
8. Wisplinghoff H, Paulus T, Lugenheim M, Stefanik D, Higgins PG, Edmond MB, et al. Nosocomial bloodstream infections due to Acinetobacter baumannii, Acinetobacter pittii and Acinetobacter nosocomialis in the United States. *J Infect* 2012;**64**:282—90.
9. Karah N, Haldorsen B, Hegstad K, Simonsen GS, Sundsfjord A, Samuelsen O, et al. Species identification and molecular characterization of Acinetobacter spp. blood culture isolates from Norway. *J Antimicrob Chemother* 2011;**66**:738—44.
10. Zheng J-Y, Huang S-S, Huang S-H, Ye Jr J. Colistin for pneumonia involving multidrug-resistant Acinetobacter calcoaceticus-Acinetobacter baumannii complex. *J Microbiol Immunol Infect* 2020;**53**:854—65.
11. Jean SS, Lee YL, Liu PY, Lu MC, Ko WC, Hsueh PR. Multicenter surveillance of antimicrobial susceptibilities and resistance mechanisms among Enterobacterales species and non-fermenting Gram-negative bacteria from different infection sources in Taiwan from 2016 to 2018. *J Microbiol Immunol Infect* 2022;**55**:463—73.
12. Chen HY, Yang YS, Hsu WJ, Chou YC, Huang LS, Wang YC, et al. Emergence of carbapenem-resistant Acinetobacter nosocomialis strain ST410 harbouring plasmid-borne blaOXA-72 gene in Taiwan. *Clin Microbiol Infect* 2018;**24**:1023—4.
13. Michalopoulos A, Falagas ME. Treatment of acinetobacter infections. *Expet Opin Pharmacother* 2010;**11**:779—88.
14. Sy CL, Chen PY, Cheng CW, Huang LJ, Wang CH, Chang TH, et al. Recommendations and guidelines for the treatment of infections due to multidrug resistant organisms. *J Microbiol Immunol Infect* 2022;**55**:359—86.
15. Chen FJ, Huang WC, Liao YC, Wang HY, Lai JF, Kuo SC, et al. Molecular epidemiology of emerging carbapenem resistance in acinetobacter nosocomialis and acinetobacter pittii in taiwan, 2010 to 2014. *Antimicrob Agents Chemother* 2019:63.
16. Yang YS, Lee YT, Wang YC, Chiu CH, Kuo SC, Sun JR, et al. Molecular epidemiology of carbapenem non-susceptible Acinetobacter nosocomialis in a medical center in Taiwan. *Infect Genet Evol* 2015;**31**:305—11.
17. Liang-Yu C, Kuo SC, Liu CY, Luo BS, Huang LJ, Lee YT, et al. Difference in imipenem, meropenem, sulbactam, and colistin nonsusceptibility trends among three phenotypically undifferentiated Acinetobacter baumannii complex in a medical center in Taiwan, 1997-2007. *J Microbiol Immunol Infect* 2011;**44**:358—63.
18. Liu PY, Ko WC, Lee WS, Lu PL, Chen YH, Cheng SH, et al. In vitro activity of cefiderocol, cefepime/enmetazobactam, cefepime/zidebactam, eravacycline, omadacycline, and other comparative agents against carbapenem-non-susceptible Pseudomonas aeruginosa and Acinetobacter baumannii isolates associated from bloodstream infection in Taiwan between 2018-2020. *J Microbiol Immunol Infect* 2022;**55**:888—95.
19. Schooley RT, Biswas B, Gill JJ, Hernandez-Morales A, Lancaster J, Lessor L, et al. Development and use of personalized bacteriophage-based therapeutic cocktails to treat a patient with a disseminated resistant acinetobacter baumannii infection. *Antimicrob Agents Chemother* 2017;**61**.
20. Principi N, Silvestri E, Esposito S. Advantages and limitations of bacteriophages for the treatment of bacterial infections. *Front Pharmacol* 2019;**10**:513.
21. Loc-Carrillo C, Abedon ST. Pros and cons of phage therapy. *Bacteriophage* 2011;**1**:111—4.
22. Skurnik M, Pajunen M, Kiljunen S. Biotechnological challenges of phage therapy. *Biotechnol Lett* 2007;**29**:995—1003.
23. Koskella B, Meaden S. Understanding bacteriophage specificity in natural microbial communities. *Viruses* 2013;**5**:806—23.

24. Gupta R, Prasad Y. Efficacy of polyvalent bacteriophage P-27/HP to control multidrug resistant Staphylococcus aureus associated with human infections. *Curr Microbiol* 2011;**62**:255—60.
25. Clokie MR, Millard AD, Letarov AV, Heaphy S. Phages in nature. *Bacteriophage* 2011;**1**:31—45.
26. Ding C, He J. Effect of antibiotics in the environment on microbial populations. *Appl Microbiol Biotechnol* 2010;**87**: 925—41.
27. Chhibber S, Kaur T, Sandeep K. Co-therapy using lytic bacteriophage and linezolid: effective treatment in eliminating methicillin resistant Staphylococcus aureus (MRSA) from diabetic foot infections. *PLoS One* 2013;**8**:e56022.
28. Jiang L, Tan J, Hao Y, Wang Q, Yan X, Wang D, et al. Isolation and characterization of a novel myophage Abp9 against pandrug resistant acinetobacater baumannii. *Front Microbiol* 2020;**11**:506068.
29. Morozova VV, Vlassov VV, Tikunova NV. Applications of bacteriophages in the treatment of localized infections in humans. *Front Microbiol* 2018;**9**:1696.
30. Miliutina LN, Vorotyntseva NV. [Current strategy and tactics of etiotropic therapy of acute intestinal infections in children]. *Antibiot Khimioter* 1993;**38**:46—53.
31. Babalova EG, Katsitadze KT, Sakvarelidze LA, Imnaishvili N, Sharashidze TG, Badashvili VA, et al. [Preventive value of dried dysentery bacteriophage]. *Zh Mikrobiol Epidemiol Immunobiol* 1968;**45**:143—5.
32. Sulakvelidze A, Alavidze Z, Morris Jr JG. Bacteriophage therapy. *Antimicrob Agents Chemother* 2001;**45**:649—59.
33. Lam HYP, Lai MJ, Chen TY, Wu WJ, Peng SY, Chang KC. Therapeutic effect of a newly isolated lytic bacteriophage against multi-drug-resistant cutibacterium acnes infection in mice. *Int J Mol Sci* 2021:22.
34. van der Heijden J, Vogt SL, Reynolds LA, Peña-Díaz J, Tupin A, Aussel L, et al. Analysis of bacterial survival after exposure to reactive oxygen species or antibiotics. *Data Brief* 2016;**7**: 894—9.
35. Schmelcher M, Donovan DM, Loessner MJ. Bacteriophage endolysins as novel antimicrobials. *Future Microbiol* 2012;**7**: 1147—71.
36. Briers Y, Lavigne R. Breaking barriers: expansion of the use of endolysins as novel antibacterials against Gram-negative bacteria. *Future Microbiol* 2015;**10**:377—90.
37. Hernandez-Morales AC, Lessor LL, Wood TL, Migl D, Mijalis EM, Cahill J, et al. Genomic and biochemical characterization of acinetobacter podophage petty reveals a novel lysis mechanism and tail-associated depolymerase activity. *J Virol* 2018; **92**.
38. Abedon ST. Selection for bacteriophage latent period length by bacterial density: a theoretical examination. *Microb Ecol* 1989; **18**:79—88.
39. Yuan Y, Li X, Wang L, Li G, Cong C, Li R, et al. The endolysin of the Acinetobacter baumannii phage vB_AbaP_D2 shows broad antibacterial activity. *Microb Biotechnol* 2021;**14**: 403—18.
40. Park DW, Park JH. Characterization of endolysin LysECP26 derived from rV5-like phage vB_EcoM-ECP26 for inactivation of Escherichia coli O157:H7. *J Microbiol Biotechnol* 2020;**30**: 1552—8.
41. Imanishi I, Uchiyama J, Tsukui T, Hisatsune J, Ide K, Matsuzaki S, et al. Therapeutic potential of an endolysin derived from kayvirus S25-3 for staphylococcal impetigo. *Viruses* 2019:11.
42. Caflisch KM, Patel R. Implications of bacteriophage- and bacteriophage component-based therapies for the clinical microbiology laboratory. *J Clin Microbiol* 2019;**57**.
43. Höltje JV. Bacterial lysozymes. *EXS* 1996;**75**:65—74.

Appendix A. Supplementary data

Supplementary data to this article can be found online at https://doi.org/10.1016/j.jmii.2023.07.012.